RSC Advances

PAPER

View Article Online
View Journal | View Issue

Cite this: *RSC Adv.*, 2018, **8**, 6502

Structural changes, thermodynamic properties, ^{1}H magic angle spinning NMR, and ^{14}N NMR of $(NH_4)_2CuCl_4 \cdot 2H_2O$

Ae Ran Lim *[ab] and Sun Ha Kim[cd]

The structural changes and thermodynamic properties of $(NH_4)_2CuCl_4 \cdot 2H_2O$ were studied by differential scanning calorimetry (DSC) and thermogravimetric (TG) analysis. In addition, the chemical shift, line width, and spin-lattice relaxation time of the crystals were also investigated by ^{1}H magic angle spinning nuclear magnetic resonance (MAS NMR), focusing on the role of NH_4 and H_2O near the phase transition temperature. The change at T_{C2} (=406 K) and T_{C3} (=437 K) seems to be a chemical change caused by thermal decomposition rather than a physical change such as a structural phase transition. The changes in the temperature dependence of these data near T_{C2} are related to variations in the environments surrounding NH_4 and H_2O. The ^{14}N NMR spectrum is also measured in order to investigate local phenomena related to the phase transition.

Received 7th January 2018
Accepted 2nd February 2018

DOI: 10.1039/c8ra00170g

rsc.li/rsc-advances

I. Introduction

A number of compounds with the chemical formula $A_2BX_4 \cdot 2H_2O$, where A = NH_4, K, Rb, Cs and B = Cu, Mn, Ca, Ni are monovalent and divalent metal ions, respectively, and X = Cl, Br is a halide ion, crystallize as perovskite-type two-dimensional layered structures.[1–7] Crystals with this arrangement can be divided into two classes according to their symmetry and structure.[8–10] The first class includes compounds containing Cu^{2+} ions that crystallize with tetragonal symmetry with the space group $P4_2/mnm$ at room temperature. The tetrahedrons surrounding the divalent metal ions placed at the corners of the unit cell are rotated by exactly 90° with respect to the tetrahedron surrounding the ion at the center of the cell. The A^{+} ions are placed in the almost cubic cavities formed by the tetrahedrons.[11,12] Crystals containing Mn^{2+}, Ca^{2+}, and Ni^{2+} ions form the second of these two classes with triclinic symmetry and the space group P_1. The $(NH_4)_2CuCl_4 \cdot 2H_2O$ crystal, which is an example of the former, exhibits a structural phase transition from the point group 4/*mmm* to the point group 4(bar)2*m* at 200 K.[13–15] In addition, two different phase transitions at approximately 383 K and 413 K were observed in the DC electric conductivity measurements reported by Narsimlu *et al.*[16] At room temperature, $(NH_4)_2CuCl_4 \cdot 2H_2O$ forms a tetragonal structure with space group $P4_2/mnm$, as shown in Fig. 1.[14] The unit cell contains two formula units and has the lattice constants $a = b = 7.596$ Å, $c = 7.976$ Å.[17] The unit cell contains two Cu^{2+} ions at equivalent positions (0, 0, 0) and (1/2, 1/2, 1/2) each surrounded by an approximate octahedron of four Cl^{-} ions and two water molecules. The line connecting the water molecules is parallel to the crystallographic *c*-axis.[1] The water molecule is trigonal coordinated and forms two equivalent O–

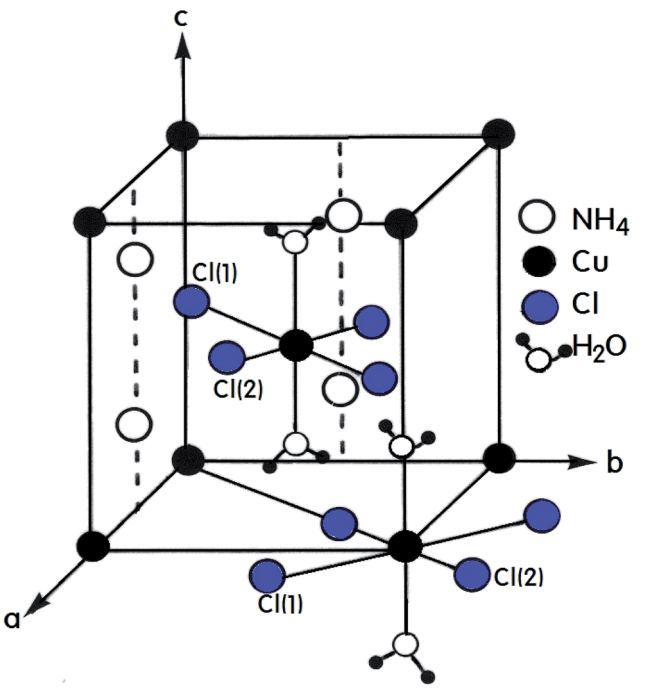

Fig. 1 Tetragonal structure of the $(NH_4)_2CuCl_4 \cdot 2H_2O$ crystal.

[a]*Analytical Laboratory of Advanced Ferroelectric Crystals, Jeonju University, Jeonju 55069, South Korea. E-mail: aeranlim@hanmail.net; arlim@jj.ac.kr; Fax: +82-63-220-2053; Tel: +82-63-220-2514*

[b]*Department of Science Education, Jeonju University, Jeonju 55069, South Korea*

[c]*Seoul Western Center, Korea Basic Science Institute, Seoul 03759, South Korea*

[d]*Department of Chemistry, Kyungpook National University, Daegu 41566, South Korea*

H···Cl(1) hydrogen bonds with an H···Cl(1) length of 2.186 Å. The O–H distance in the water molecule is 0.965 Å. The NH_4^+ is hydrogen bonded to the Cl(1) atoms at 3.357 Å, while in the other orientation, it is bonded to the Cl(2) atoms at 3.370 Å. The respective N–H distances are 1.011 Å and 1.021 Å.[17]

The purpose of this study is to investigate the structural changes and thermodynamic properties of $(NH_4)_2CuCl_4\cdot 2H_2O$ single crystals using differential scanning calorimetry (DSC) and thermogravimetric (TG) analysis. Further, the chemical shift, line width, and spin-lattice relaxation time $T_{1\rho}$ in the rotating frame of $(NH_4)_2CuCl_4\cdot 2H_2O$ are measured by ^1H magic angle spinning/nuclear magnetic resonance (MAS/NMR) near the phase transition temperature, focusing on the role of NH_4 and H_2O. In addition, the ^{14}N NMR spectrum in the laboratory frame is measured as a function of the temperature, in an attempt to understand the structural geometry near the phase transition temperature. Our findings represent the first report on the thermodynamic properties and NMR characteristics of $(NH_4)_2CuCl_4\cdot 2H_2O$, and are useful for understanding the phase transitions.

II. Experimental method

Single crystals of $(NH_4)_2CuCl_4\cdot 2H_2O$ were grown by slowly evaporating aqueous solutions containing a stoichiometric mixture of NH_4Cl and $CuCl_2\cdot 2H_2O$ in the molar ratio of 2 : 1 at room temperature. The obtained crystals were light blue. The phase transition temperature was determined using a Dupont 2010 DSC instrument. The rate of temperature change during heating was 10 °C min^{-1}.

The ^1H MAS NMR spectra of $(NH_4)_2CuCl_4\cdot 2H_2O$ in a rotating frame were obtained using the Bruker DSX 400 FT NMR spectrometer at the Korea Basic Science Institute, Western Seoul Center. The static magnetic field used was 9.4 T, and the central radio frequency was set at $\omega_0/2\pi$ = 400.13 MHz for the ^1H nucleus. The powder sample was placed in a 4 mm MAS probe, and the MAS rate was set to 5 kHz to minimize spinning sideband overlap. The spin-lattice relaxation times in the rotating frame were measured using a saturation recovery pulse sequence called sat–t–$\pi/2$; the nuclear magnetizations of the ^1H nuclei at time t after the sat pulse, a combination of one hundred $\pi/2$ pulses applied at regular intervals, were determined following the $\pi/2$ excitation pulse. The width of the $\pi/2$ pulse was 3.45 μs below 410 K and 6.7 μs above 420 K for ^1H.

In addition, the ^{14}N NMR spectra of the $(NH_4)_2CuCl_4\cdot 2H_2O$ single crystals in the laboratory frame were measured using a Unity INOVA 600 NMR spectrometer at the Korea Basic Science Institute, Western Seoul Center. The static magnetic field was 14.1 T, and the Larmor frequency was set to $\omega_0/2\pi$ = 43.342 MHz. The ^{14}N NMR experiments were performed using the solid-state echo sequence: 3.7 μs–t–3.7 μs–t. The NMR measurements were obtained in the temperature range of 180–430 K. Unfortunately, the chemical shift and resonance frequency could not be measured above 430 K because the NMR spectrometer did not have adequate temperature control at high temperature. The temperatures of all the samples were maintained at constant values by controlling the helium gas flow and heater current, which yielded an accuracy of ±0.5 K.

III. Results and discussion

The structure of the $(NH_4)_2CuCl_4\cdot 2H_2O$ crystals at room temperature was determined by X-ray diffraction (XRD) (PANalyical, X'pert Pro MPD) with a Cu-Kα (λ = 1.5418 Å) radiation source at the Korea Basic Science Institute, Western Seoul Center. Measurement was taken in a θ–2θ geometry from 10° to 60° at 45 kV and 40 mA tube power. The $(NH_4)_2CuCl_4\cdot 2H_2O$ crystals were determined to have a tetragonal structure with the lattice constants $a = b$ = 7.5991 Å, c = 7.9661 Å, $\alpha = \beta = \gamma = 90°$. This result is consistent with those of previous studies.[1,17] The DSC analysis of the $(NH_4)_2CuCl_4\cdot 2H_2O$ crystals revealed three endothermic peaks during heating, as shown in Fig. 2. The mass of the powdered samples used in the DSC experiment is 6.6 mg. The endothermic peak enlarged in Fig. 2 near 200 K ($=T_{C1}$) is consistent with the phase transition temperature reported previously, and is very small relative to the other endothermic peaks. The endothermic peaks near 406 K ($=T_{C2}$) and 437 K ($=T_{C3}$) are related to the thermal dehydration according to the below-mentioned loss of H_2O. TG analysis was used to determine whether these high-temperature transformations were structural phase transitions or melting temperatures. The TG curve of $(NH_4)_2CuCl_4\cdot 2H_2O$ is shown in Fig. 3. The first occurrence of mass loss begins at approximately 364 K, and at 406 K, 96.75% of mass remains, yielding $(NH_4)_2CuCl_4\cdot 1.5H_2O$. The mass loss at 430 K and 437 K reaches 6.49% and 9.74% for $(NH_4)_2CuCl_4\cdot H_2O$ and $(NH_4)_2CuCl_4\cdot 0.5H_2O$, respectively. The bulk mass of $(NH_4)_2CuCl_4\cdot 2H_2O$ decreases at 364 K (T_d), which is ascribed to the onset of partial thermal decomposition, and reaches complete thermal decomposition, thereby turning into $(NH_4)_2CuCl_4$, at approximately 443 K. The transformation anomalies at 406 ($=T_{C2}$) and 437 K ($=T_{C3}$) in the DSC experiment are related to the phase transitions from $(NH_4)_2CuCl_4\cdot 2H_2O$ to $(NH_4)_2CuCl_4\cdot 1.5H_2O$ and from $(NH_4)_2CuCl_4\cdot 2H_2O$ to $(NH_4)_2CuCl_4\cdot 0.5H_2O$, respectively.

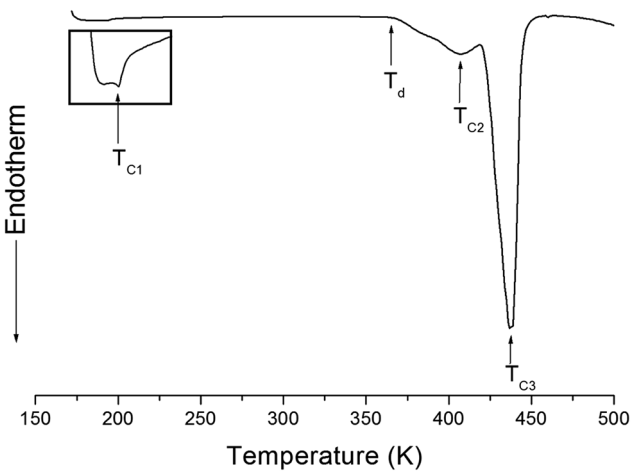

Fig. 2 DSC thermogram of $(NH_4)_2CuCl_4\cdot 2H_2O$ upon heating.

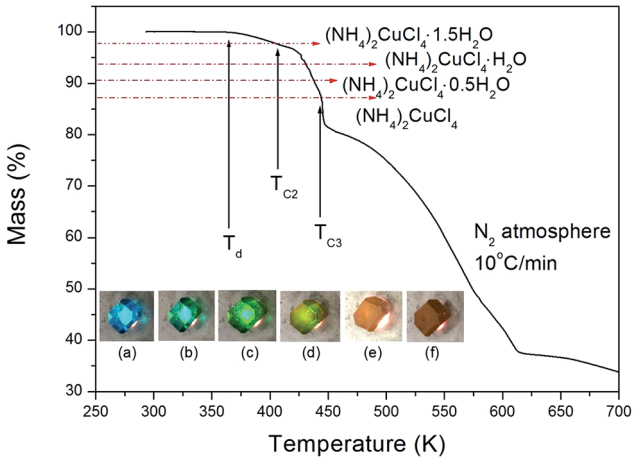

Fig. 3 Thermogravimetric analysis (TGA) of $(NH_4)_2CuCl_4 \cdot 2H_2O$ (inset: color changes according to the temperature: (a) 295 K, (b) 373 K, (c) 386 K, (d) 393 K, (e) 433 K, and (f) 448 K).

Optical polarizing microscopy showed that the crystals are light blue in color at room temperature and that they undergo color changes as the temperature increases. As the temperature increases, the color of the crystal varies from light blue (295 K and 373 K) to light green (386 K) to green (393 K) to dark yellow (433 K) and finally to brown (448 K), as shown in the inset of Fig. 3. This color change may be related to the partial loss of H_2O. The DSC peaks at 406 K and 437 K are related to chemical changes through thermal dehydration, based on the TG and optical polarizing microscopy results. The weight loss evidenced by the TG curve suggests that T_{C2} and T_{C3} in $(NH_4)_2CuCl_4 \cdot 2H_2O$ are not related to physical changes such as structural phase transitions. Rather, they are related to a chemical change through thermal dehydration.

The ^{1}H MAS NMR spectra of $(NH_4)_2CuCl_4 \cdot 2H_2O$, which were obtained as a function of temperature, only exhibit one peak ascribed to chemical shift, as shown in Fig. 4. The spinning sidebands of the peak are marked with asterisks. There are two kinds of protons in $(NH_4)_2CuCl_4 \cdot 2H_2O$: ammonium protons and water protons. The current experiment was unable to distinguish the signals resulting from these two types of protons, because the eight protons from ammonium and the four protons from water are expected to yield two superimposed lines. Thus, the signal generated by the ammonium protons might include the signal caused by the water protons.

The chemical shifts for the ^{1}H nuclei in $(NH_4)_2CuCl_4 \cdot 2H_2O$ with respect to tetramethylsilane (TMS) at a frequency of 400.13 MHz are presented in Fig. 5 as a function of temperature. The chemical shifts of the ^{1}H nucleus change abruptly near T_{C2}, whereas those near T_{C1} are continuous. The change in the chemical shift with temperature indicates that the configuration of the atoms neighboring the ^{1}H nuclei is undergoing change. The full width at half maximum (FWHM) of the ^{1}H MAS NMR signal is shown in the inset of Fig. 5 as a function of temperature. As the temperature increases, the FWHM near T_{C1} is continuous, and that near T_{C2} decreases in a step-like shape. This stepwise narrowing is generally considered to be caused by internal motions, which have a temperature dependence related to that observed for the chemical shift. The shape of the line changes progressively with increasing temperature from the Gaussian-like shape of a rigid lattice to a Lorentzian shape. Near T_{C2} the line width undergoes an abrupt drop, after which the line width becomes considerably narrower.

The nuclear magnetization recovery traces for ^{1}H MAS NMR are usually represented by a single-exponential function. However, the magnetization recovery traces for ^{1}H MAS NMR in $(NH_4)_2CuCl_4 \cdot 2H_2O$ could be described by the following double-exponential function:[18–20]

$$M(t)/M(\infty) = a \exp(-t/T_{1\rho}(s)) + b \exp(-t/T_{1\rho}(l)), \quad (1)$$

where $T_{1\rho}(s)$ and $T_{1\rho}(l)$ are the short and long spin-lattice relaxation times, respectively. The magnetization recovery

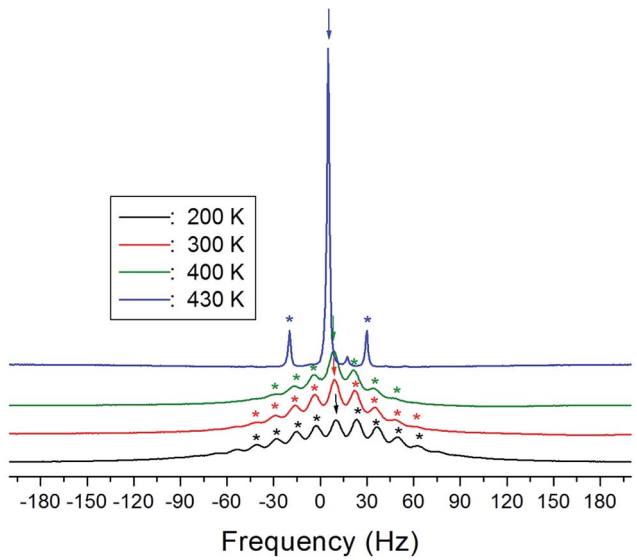

Fig. 4 ^{1}H MAS NMR spectrum of $(NH_4)_2CuCl_4 \cdot 2H_2O$ at several temperatures.

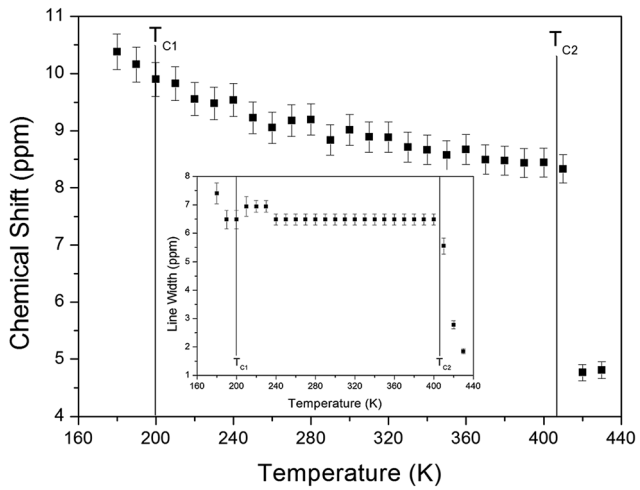

Fig. 5 Chemical shift of ^{1}H MAS NMR spectrum of $(NH_4)_2CuCl_4 \cdot 2H_2O$ as a function of temperature. (inset: line width of the ^{1}H MAS NMR spectrum of $(NH_4)_2CuCl_4 \cdot 2H_2O$).

traces showing the delay time of the ^{1}H resonance signal at temperatures of 200 K, 420 K, and 430 K are shown in the inset of Fig. 6. The obtained spin-lattice relaxation curves were well fitted by the abovementioned double-exponential function, with the slope of the recovery trace decreasing as the temperature increased. Note that the occurrence of a double-exponential spin-lattice relaxation pattern is unusual for a strongly dipolar-coupled proton system, whereas spin diffusion is expected to afford a single-exponential relaxation pattern.[21] Therefore, we concluded that the proton system comprises two spatially well-separated nuclei. The values of $T_{1\rho}$ for ^{1}H in $(NH_4)_2CuCl_4\cdot 2H_2O$ at several temperatures are shown in Fig. 6. As mentioned above, two different sets of $T_{1\rho}$ values were obtained from the double-exponential function: the larger values, $T_{1\rho}(l)$, correspond to the longer N–H$\cdots$Cl chain systems in the NH_4 groups, whereas the smaller ones, $T_{1\rho}(s)$, correspond to the shorter O–H$\cdots$Cl chain systems in the H_2O groups. Here, $T_{1\rho}(l)$ decreases slightly with increasing temperature, as opposed to $T_{1\rho}(s)$, which increases with increasing temperature. Furthermore, $T_{1\rho}(s)$ and $T_{1\rho}(l)$ for ^{1}H in these groups were continuous in close proximity to T_{C1}, whereas $T_{1\rho}(s)$ and $T_{1\rho}(l)$ of ^{1}H in both the H_2O and NH_4 groups were discontinuous close to T_{C2}, corresponding to an abrupt increase with increasing temperature. The abrupt rise in $T_{1\rho}$ near T_{C2} contributes to the increased mobility of the protons in H_2O and NH_4. The changes observed for the ^{1}H nucleus near T_{C2} are related to variations in the symmetry of the environments of H, *i.e.*, to changes in the symmetry of the NH_4 and H_2O groups. The forms of the tetrahedrons of water molecules are probably disrupted by the loss of H_2O.

The NMR spectra of ^{14}N of $(NH_4)_2CuCl_4\cdot 2H_2O$ single crystals were recorded in order to investigate local phenomena related to the phase transition. The ^{14}N nucleus has a spin number 1. Spectra were obtained by the solid-state echo method using static NMR at a Larmor frequency of $\omega_0/2\pi = 43.342$ MHz in the laboratory frame. The ^{14}N NMR spectra of $(NH_4)_2CuCl_4\cdot 2H_2O$ single crystals at 200, 300, and 400 K are shown in Fig. 7. Two resonance lines are expected because of the quadrupole interaction of the ^{14}N ($I = 1$) nucleus.[19] With respect to the crystal orientation, the magnetic field was applied along the crystallographic *c*-axis. The resonance frequencies of the ^{14}N signals are plotted in Fig. 8, as a function of temperature. In the vicinity of T_{C1}, the frequencies of both signals are discontinuous, whereas those near T_{C2} are continuous, and the resonance frequency increases with increasing temperature. In addition, the splitting of the ^{14}N resonance lines above 200 K increases slightly with increasing temperature. These temperature-dependent changes in the ^{14}N resonance frequencies are attributed to changes in the structural geometry of the NH_4^+ ion.[22] In all temperature, all nitrogen is physically equivalent, and the ^{14}N quadrupole parameter is slowly increased.[23] In this case, the electric field gradient (EFG) tensors at the N sites are varied, reflecting the changing atomic configurations around the ^{14}N nuclei in NH_4.

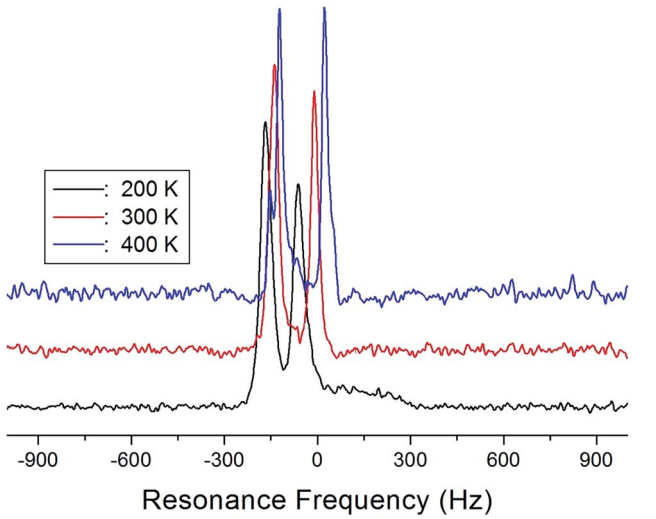

Fig. 7 ^{14}N NMR spectrum of a $(NH_4)_2CuCl_4\cdot 2H_2O$ single crystal at 200 K, 300 K, and 400 K.

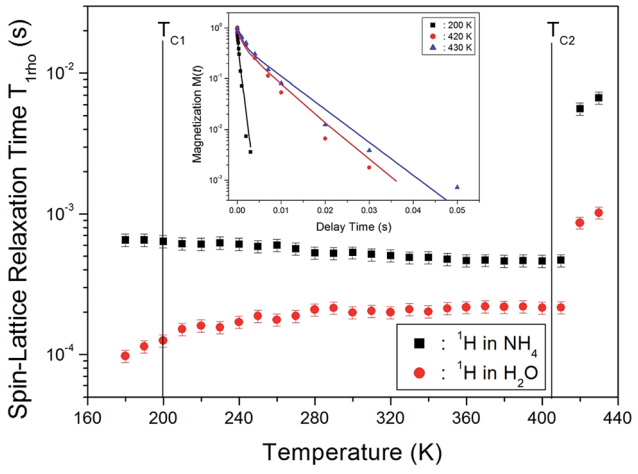

Fig. 6 Temperature dependences of the ^{1}H spin-lattice relaxation time in the rotating frame, $T_{1\rho}(s)$ and $T_{1\rho}(l)$ for H_2O and NH_4 in $(NH_4)_2CuCl_4\cdot 2H_2O$ (inset: the saturation recovery traces for delay time for ^{1}H in $(NH_4)_2CuCl_4\cdot 2H_2O$).

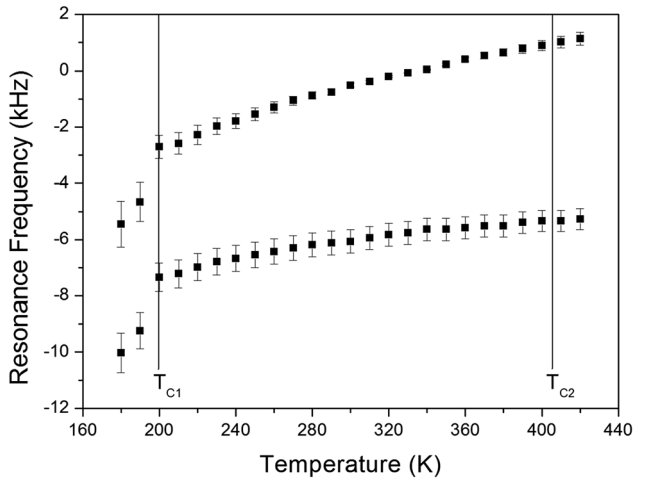

Fig. 8 Resonance frequencies of ^{14}N NMR spectrum of a $(NH_4)_2CuCl_4\cdot 2H_2O$ single crystal as a function of temperature.

IV. Conclusion

The thermodynamic properties and structural mechanisms near the phase transition temperatures in $(NH_4)_2CuCl_4 \cdot 2H_2O$ were studied through DSC, TG, NMR chemical shift, and the spin-lattice relaxation time $T_{1\rho}$. The DSC and TG results indicate that the endothermic peak near 200 K ($=T_{C1}$) is a structural phase transition, and the endothermic peaks near 406 K ($=T_{C2}$) and 437 K ($=T_{C3}$) are related to a chemical change through thermal dehydration due to the escape of H_2O. On the other hand, the changes in the temperature dependence of the chemical shift, linewidth, and spin-lattice relaxation time $T_{1\rho}$ near T_{C2} are related to variations in the symmetry of the environments of NH_4 and H_2O. The mechanism of these changes at high temperature is related to hydrogen bond proton transfer involving the breakage of a weak hydrogen bond. The change at T_{C2} and T_{C3} seems to be a chemical change caused by thermal decomposition rather than a physical change such as a structural phase transition, and the tetrahedrons formed by the water molecules are probably disrupted by the loss of H_2O. From the DSC, TG, and NMR data, it is clear that the structural change at high temperature arises due to the loss of the two water molecules coordinated to the Cu^{2+} ion along the *c*-axis.

Conflicts of interest

There are no conflicts to declare.

Acknowledgements

This research was supported by the Basic Science Research program through the National Research Foundation of Korea (NRF), funded by the Ministry of Education, Science and Technology (2016R1A6A1A03012069 and 2015R1A1A3A04001077).

References

1 N. Narsimlu and K. S. Kumar, *Cryst. Res. Technol.*, 2002, **37**, 945.
2 Z. Tylczynski, M. Wiesner and A. Trzaskowska, *Phys. B*, 2016, **500**, 85.
3 A. R. Lim and J. Cho, *J. Mol. Struct.*, 2017, **1146**, 324.
4 T. O. Klaassen and N. J. Poulis, *J. Phys. Colloq.*, 1971, **32**(C1), 1157.
5 V. E. Zavodnik, V. K. Bel'skii, I. Diaz and V. Fernandez, *Crystallogr. Rep.*, 1999, **44**, 575.
6 W. Kaminsky, S. Haussuhl, A. Brandstadtor and C. Balarew, *Z. Kristallogr.*, 1994, **209**, 395.
7 V. D. Franke, Y. O. Punin and L. A. P'yankova, *Crystallogr. Rep.*, 2007, **52**, 349.
8 M. Czlonkowska, Z. Tylczynski and M. Laniecki, *Cryst. Res. Technol.*, 2006, **41**, 464.
9 V. Stefov and B. Soptrajanov, *Vib. Spectrosc.*, 1999, **19**, 431.
10 S. N. Bhakay-Tamhane, A. Sequeira and R. Chidanbaram, *Acta Crystallogr., Sect. B: Struct. Crystallogr. Cryst. Chem.*, 1980, **36**, 2925.
11 R. Chidambaram, Q. O. Navarro, A. Garcia, K. Linggoatmodjo, L. S. Chien and I.-H. Suh, *Acta Crystallogr., Sect. B: Struct. Crystallogr. Cryst. Chem.*, 1970, **26**, 827.
12 K. Waizumi, H. Masuda and H. Ohtaki, *Acta Crystallogr., Sect. C: Cryst. Struct. Commun.*, 1992, **48**, 1374.
13 Z. Tylczynski and M. Wiesner, *Mater. Chem. Phys.*, 2015, **149–150**, 566.
14 M. L. bansal, V. C. Sahni and A. P. Roy, *J. Phys. Chem. Solids*, 1979, **40**, 109.
15 H. Suga, M. Sorai, T. Yamanaka and S. Seki, *Bull. Chem. Soc. Jpn.*, 1965, **38**, 1007.
16 N. Narsimlu, K. Sivakumar and G. S. Sastry, *Cryst. Res. Technol.*, 1996, **31**, 385.
17 S. N. Bhakay-Tamhane, A. Sequeira and R. Chidambaram, *Acta Crystallogr., Sect. B: Struct. Crystallogr. Cryst. Chem.*, 1980, **36**, 2925.
18 J. L. Koenig, *Spectroscopy of Polymers*, Elsevier, New York, 1999.
19 A. Abragam, *The Principles of Nuclear Magnetism*, Oxford University Press, 1961.
20 B. Cowan, *Nuclear Magnetic Resonance and Relaxation*, Cambridge University, UK, 1997.
21 A. R. Lim, S. W. Kim and Y. L. Joo, *J. Appl. Phys.*, 2017, **121**, 215501.
22 A. R. Lim, *Solid State Sci.*, 2016, **52**, 37.
23 J. Seliger, R. Blinc, H. Arend and R. Kind, *Z. Phys., B, Condens. matter*, 1976, **25**, 189.